

QUANTUM MECHANICAL COMPUTATION AND MOLECULAR DOCKING ANALYSIS OF 7-HYDROXYCHROMEN-2-ONE

M. Ramraj^{1*} and K. Santhi²

¹ Dept of Physics, Periyar University PG Extn Centre, Dharmapuri, India

² Dept of Physics, Thiagarajar Polytechnic college, Salem, India

Corresponding author email id*: ramrajparvathi977@gmail.com

ABSTRACT

The Umbelliferone (UMB) molecule was optimized by density functional theory with B3LYP/6-311G (d,p) and HF /6-311G (d, p) basis set. The time-dependent DFT method was engaged to calculate the Frontier Molecular orbitals (FMOs) of the UMB molecule. The reactivity and selectivity of UMB are analyzed using parameters like MEP, global reactivity descriptors, Fukui function. Mulliken atomic charges are calculated and interpreted. The TDOS, PDOS and OPDOS of the molecule have been plotted and interpreted. Thermodynamic properties of the title molecule calculated. The molecular docking analysis reveals that inhibitory nature of the UMB molecule is a proved inhibitor of the PI3K inhibitor activity.

Keywords: DFT, HF, HOMO–LUMO, Fukui function

INTRODUCTION

Umbelliferone name is from the umbelliferae group of plants, and the plant family thusly was named for their umbrella-molded inflorescences, each called an umbel [1]. Umbelliferone (7-hydroxycoumarin) is the one the most well-known compound of the coumarin family. This compound gets the consideration of researchers because of its assorted bioactivities in various applications in different remedial fields [2]. An intriguing part of umbelliferone is auxiliary obligation. Umbelliferone, generally called 7-hydroxycoumarin, hydrangine, skimmetine, and beta-umbelliferone, is a trademark consequence of the coumarin family. The IUPAC name of UMB is 7-Hydroxychromen-2-one. It appears in Yellowish-white crystalline odorless powder. The molecular formula is C₉H₆O₃. The biological activities have been evaluated as potential inhibitor

of the PI3K inhibitor [3,4]

DFT and HF methods has been a favorites one due to its better accuracy in reproducing the molecular geometry, atomic charges, dipolemoment,thermodynamic properties [5] etc. The literature survey reveals that so far there is no complete theoretical study for the title molecule.The present study aims to give a complete description of the molecular geometry and electronic properties of the UMBmolecule. Frontier molecular orbitals (FMOs) of the title molecule have been analyzed used to elucidate information regarding charge transfer in the molecule. The local reactivity descriptors like local softness and electrophilicity indices were obtained with the help of Fukui function calculation [6].The Milliken Population analyses of the title compound have been calculated and the calculated values have been reported. Thermodynamic properties and DOS, OPDOS and PDOS have been calculated and interpreted.All the basic calculations were performed using the Gaussian 09 software program.

Materials and methods

Computational details

The spectroscopic analysis and the quantum chemical calculations of the title compound were calculated using B3LYP (Becke 3-Lee-Yangand Parr) and HF level of theories in Gaussian 09 software package with6-311G (d,p) basis set [7]. The optimized structure, the molecular geometry and the MEP diagramwas visualized using Gauss View 5.0 software program [8]. Frontier Molecular Orbitals (FMOs) and Fukui function,local softness and electrophilic indices were calculated from Mullikenatomic charge of title molecule using the same level of theory.The totaldensity of states (TDOS), overlap population density of states (OPDOS)and the partial density of states (PDOS) spectra were calculated utilizing Gauss Sum2.2 program [9,10]. The molecular docking analysis was performed with Autodock 4.2 and cygwin software package. The protein–ligand complex and intermolecular interactions between the protein and ligand molecule were viewed with the PyMOL [11], Chimera [12].

RESULTS AND DISCUSSION

Optimized geometry

The molecular structure of UMB belongs to C1 point group and optimized structure of the molecule is viewed using Gauss view software. Figure 1 shows the ball and stick model of optimized structure of UMB. The geometrical parameters (bond lengths, bond angles and Torsion angles) of the title molecule were calculated by DFT method using the basis sets B3LYP

/6-311G (d, p) and HF /6-311G (d, p). The HF/6-311G (d, p) basis set value is more accurate than B3LYP (6-311G (d, p)) basis set. The molecule has twenty seven C-C bonds, twenty four C-H bonds, thirteen C-O bonds, two O-H are presented in Table 1. The C-C bond distance of aromatic ring ranges from 1.276 to 1.383 Å, and the average value is 1.343 Å. On comparing the torsion angle values of the bonds C(1)-C(2)-C(3)-H(14), C(4)-C(5)-C(6)-H(16), O(10)-C(1)-C(2)-H(13) and O(11)-C(1)-O(10)-C(9) are higher values in active site when compared with Gas phase due to intermolecular interactions of the UMB molecule. On comparing the torsional angle values of the bonds C(3)-C(4)-C(9)-O(10), C(4)-C(5)-C(6)-C(7) and H(15)-C(5)-C(6)-H(16) are lower values in active site when compared with Gas phase due to intermolecular interactions of the UMB molecule.

Molecular electrostatic potential

Molecular electrostatic potential (MEP) Electrostatic potential maps, also known as electrostatic potential energy maps, or molecular electrical potential surfaces, characterize the charge distributions of molecules three dimensionally [13]. The purpose of finding the ESP is to find out the reactive site of a molecule. These maps allow us to visualize variably charged regions of a molecule. Recognition of the charge distributions can be used to determine how molecules interact with one another. Molecular electrostatic potential (MEP) mapping is very useful in the observation of the molecular structure with its physiochemical property relationships [14]. Total SCF electron density surface mapped with MEP of UMB are shown in Fig.2a. The molecular electrostatic potential surface MEP which is a three dimensional plot of ESP mapped on the electron density surface. Rapidly displays molecular shape, size and ESP values. The color scheme for the MEP surface have been chosen such that regions of attractive potential appear in red and those of repulsive potential appear in blue, yellow shows slightly electron rich sections. The low potential (red), are studied by an abundance of electrons [15]. The MEP of ESP map gives the information about the drug receptor interactions, and allows predicting nucleophilic and electrophilic sites of the molecule. The ESP particularly on the molecular surface gives information about, how the molecule will approach and bind with the biological receptors. The ESP map displays high electronegative regions in the vicinity of O (10), O (11) and O (12) atoms. Fig.2b. also confirms the different negative and positive potential sites of the molecule in accordance with the total electron density surface. The electrostatic

potential mapped surface are investigated and have been plotted for UMB molecule in B3LYP/6-311G (d,p) basis set using the Gauss view software.

Electronic Properties (HOMO-LUMO analysis)

The fundamental importance of the HOMO (Highest Occupied Molecular Orbital) and LUMO (Lowest Unoccupied Molecular Orbital) comprehends the substance steadiness and reactivity of numerous natural gatherings. The energy difference between HOMO and LUMO orbits called energy gap which is considered as important for indicator of compound stability. Most noteworthy involved sub-atomic orbital and least empty sub-atomic orbital are much explicit parameters of quantum science [16]. We can explain the way of component interacts with another species. Both HOMO and LUMO are important orbital taking part in chemical reaction. The ability of HOMO characterizes giving of electrons, the ability of LUMO characterizes as the accepting of electrons. Outermost orbital containing donor electrons are called HOMO; the innermost orbital contains free places to accept electrons are called LUMO. So the HOMO as a donor and LUMO as an acceptor [17-20]. The positive phase is red and the negative phase is green. The HOMO and LUMO energies of UMB molecule is -9.066494eV and -5.837790 eV respectively. The HOMO-LUMO energy difference is -3.2287 eV are shown in Figure.3. Moreover lower in the HOMO and LUMO energy gap explains the eventual charge transfer interactions taking place within the compound, which influences the biological activity of the compound and also energy serves as a measure of the excitability of the compound, the smaller the energy gap the more easily the compound will be excited. The lowering of the HOMO-LUMO band gap is a consequence of the large stabilization of the LUMO due to the strong electron-acceptor of the electron-acceptor group. By using HOMO-LUMO energies, the chemical reactivity description of molecules such as the hardness, Chemical potential, softness, electronegativity and Electrophilicity index as well the local reactivity as have been defined. Hardness (η), the ionization potential (μ) and electronegativity (χ) and softness (S) are derived as follows [5]. The calculated value of ionization potential, electron affinity and the electronegativity of UMB are presented in table 2. DFT the values are 9.0664, 5.837790, 7.45214 eV. UMB has low electronegativity as well as electron affinity when compared with the ionization potential; hence the molecule has a fewer tendencies to accept electrons.

Fukui function

The local quantities such as local softness explain by selectivity of a specific site of the molecule. The Fukui function is defined as

$$F(r) = (\partial p / \partial N) v(r) = [\delta \mu / \delta v(r)] N$$

Kolandaivel et al. [21], introduced the atomic descriptor to determine the local reactive site of the molecular system. The individual atomic charges calculated by Mullikan population analysis have been used to calculate the Fukui function [22]. The Fukui function for selected atomic sites in the UMB molecule has been listed in Table 3. Werito Yang and WilfriedJ.Moriter have given a simple procedure to calculate the atomic condensed Fukui function indices based on MPA and on three possible finite difference approximations to the derivatives.

Fukui function calculated using the following equation:

$$F^+(r) = q_r(N+1) - q_r(N) \text{ for nucleophilic attack}$$

$$F^-(r) = q_r(N) - q_r(N-1) \text{ for electrophilic attack}$$

The local softness can be represented as:

$$S_r^+ = f_r^+ / S \text{ for nucleophilic attack}$$

$$S_r^- = f_r^- / S \text{ for electrophilic attack}$$

Where +, -, 0 signs show nucleophilic and electrophilic are respectively. Table 3 shows the f_r and $(S_r f_r)$ values for the title compound, using which one can find the complexities associated with f_r values due to the negative values being removed in the $(S_r f_r)$ values.[23] The calculated f_r^+ values predict that the possible sites for nucleophilic case as (C3, C6, C9, H13, H15 and H17). The calculated f_r^- values predict that the possible sites for electrophilic case as C1, C2, C4, C5, and O10). It could therefore be concluded that the possibility of nucleophilic attack is higher than that of electrophilic attack.

Density of states (DOS)

In the boundary region, neighboring orbitals may indicate the quasi degenerate energy levels. In such cases, consideration of only the HOMO and LUMO may not yield a realistic description of the frontier orbitals. Therefore, the total (TDOS), partial (PDOS), and overlap

population (OPDOS or COOP (Crystal Orbital Overlap Population)) density of states, as terms of Mullikan population investigation are determined and created by convoluting the molecular orbital information with Gaussian curves of unit height and full width at half maximum (FWHM) of 0.3eV by utilizing the Gauss Sum 2.2 program. The TDOS, OPDOS and PDOS of the plotted in Figures [4a,4b and 4c], respectively. They give a pictorial representation of MO (molecule orbital) compositions and their commitments to chemical bonding. [24]

The most important application of the DOS plots is to demonstrate MO compositions and their contributions to the chemical bonding through the OPDOS plots which are also referred in the literature as COOP diagrams. The OPDOS shows the bonding, anti-bonding and nonbonding nature of the interaction of the two orbitals, atoms or groups. A positive value of the OPDOS indicates a bonding interaction (because of the positive overlap population), negative value means that there is an anti-bonding interaction (due to negative overlap population) and zero value indicates nonbonding interactions[25].

Furthermore, the OPDOS charts enable us to decide and look at of the giver acceptor properties of the ligands and learn the bonding, non-bonding [26]. The calculated total electronic density of states (TDOS) diagrams of the UMB is given in Figure 4a. The partial density of state plot (PDOS) mainly introduces the organization of the fragment orbitals contributing to the molecular orbitals which is seen from Figure 4b. As seen from Figure 4c, the OPDOS spectrum is shown.

Thermodynamic properties

The statically thermodynamic functions: heat capacity, entropy and enthalpy changes for the UMB molecule are obtained from the theoretical harmonic frequencies and listed in Table 4. From Table 4.it can be observed that these thermodynamic functions are increasing with temperature ranging from 100 to 1000K due to the fact that the molecular vibrational intensities increase with temperature [27]. The thermodynamics parameter such as zero point vibrational energy, thermal energy, specific heat capacity, rotational constants, entropy, dipole moment of UMB are calculates the using B3LYP /6311G (d /p) basis set Table number.4. The statistical thermo chemical analysis of UMB is carried out considering the molecule to be at room temperature of 298.15 K and one atmospheric pressure is shown in Figure.5. The correlation equation b/w heat capacities, entropies, enthalpy change and temperature were tatted by quadrat formula [28-32]. All the computed thermodynamic data is helpful for the further study on the

UMB molecule.

Molecular Docking analysis

The UMB molecule is a proved inhibitor of the PI3K inhibitor activity. The binding of this molecule to the PI3K inhibitor leads to a structural change in the PI3K inhibitor. The investigation of the structural change is responsible for the inhibition of the PI3K inhibitor. The docking analysis predicted that the lowest docked energy of the UMB molecule in the active site of PI3K inhibitor is -5.98 kcal/mol. The predicted 10 conformers and their corresponding binding energy values are listed in Table 5.

The amino acid residues involved in the intermolecular interactions with UMB molecule in the active site of PI3K inhibitor are Lys14, Lys296 and Tyr18. Among these residues the amino acids Lys297, Lys296 and Tyr18 are involved in the strong hydrogen bonding interactions with the UMB molecule at the distances 2.5, 2.4 and 2.1 Å respectively. This strongly suggests that the UMB molecule is stabilized by forming hydrogen bonding interactions with these important amino acid residues. The Lys14 amino acid forms strongest hydrogen bonding interactions with H (25) and O(12) atoms at the distance of 2.4 and 2.5 Å respectively. The intermolecular interactions formed by UMB molecule in the active site of PI3K inhibitor are shown in Figure 6a,b. The surface view of UMB molecule binding in the active site of PI3K inhibitor is shown in Figure 7. The intermolecular interactions formed by UMB in the active site of PI3K inhibitor and their nearest neighbor distances are listed in Table 6.

CONCLUSION

A complete vibrational and molecular arrangement investigation has been performed based on the quantum mechanical approach by B3LYP and HF calculations with 6-311 G(d,p) basis set. Mulliken population analysis was carried out. The calculated HOMO and LUMO energies were used to investigate the charge transfer within the molecule. The predicted MEP diagram exposed the negative regions of the molecule, was subjected to the electrophilic attack of the title compound. The orbital energy interaction between selective functional groups are investigated by density of energy states. Thermodynamic properties and Fukui function have been carried out. The present study established that the docking score for the lowest binding energy conformation of UMB is -5.98 kcal/mol. The docking investigation and quantum chemical

calculation indicates the accurate conformational and molecular orientations of UMB in the activesite of PI3K inhibitor.

Figure Caption

Fig.1 The ball-and-stick model of optimized structure of UMB with atom numbering scheme

Fig.2 a) Molecular Electrostatic potential map **b)**Contour map of UMB molecule

Fig.3 HOMO-LUMO orbitals of UMB molecule

Fig.4a) DOS, **b)** OPDOS and **c)** PDOS of UMB molecule

Fig 5.Thermodynamic propertiesof UMB molecule

Fig.6 (a,b):The intermolecular interactions formed by umbelliferone molecule in the active site of PI3K inhibitor

Fig.7 The surface view of umbelliferonemolecule binding in the active site of PI3K inhibitor

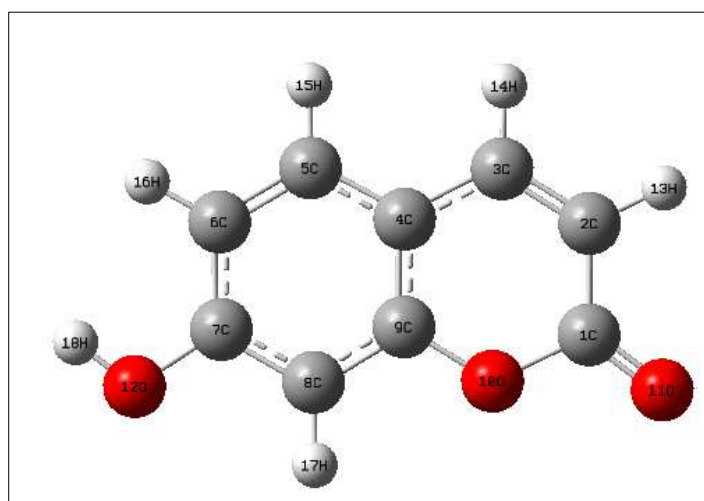
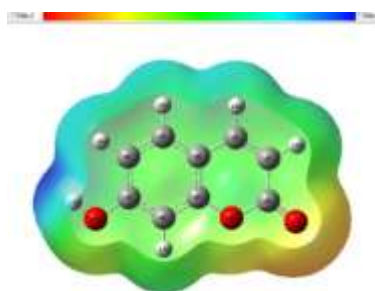
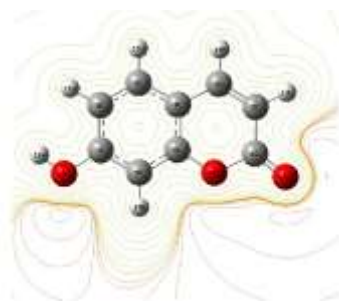


Fig. 1 The ball-and-stick model of optimized structure of UMB with atom numbering scheme



a)



b)

Fig.2 a) Molecular Electrostatic potential map **b)**Contour map of UMB molecule

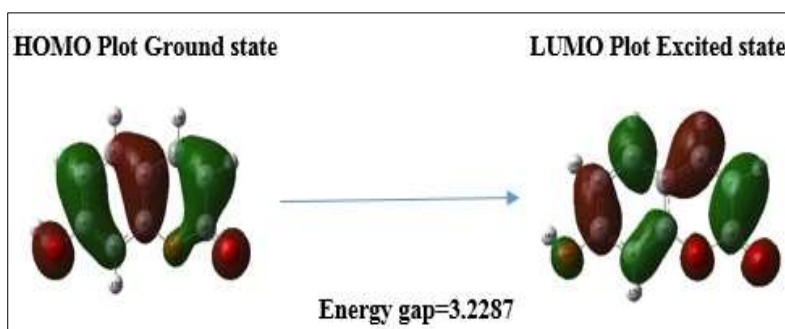
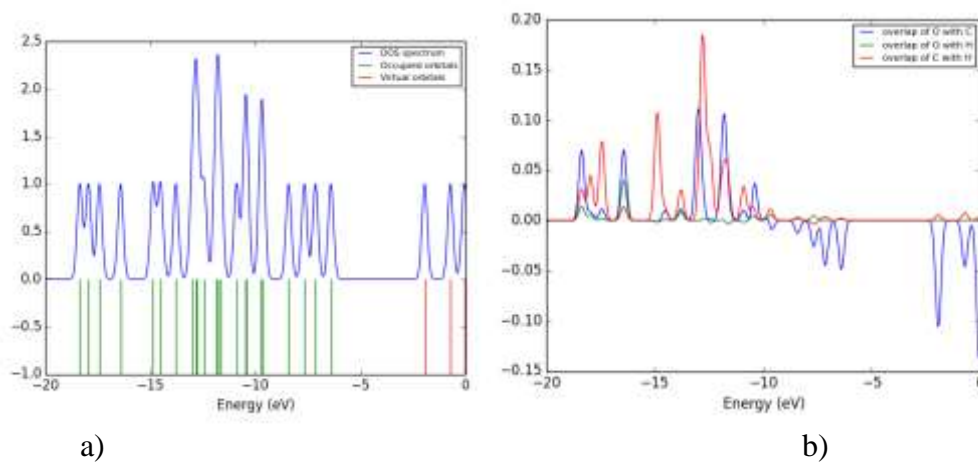
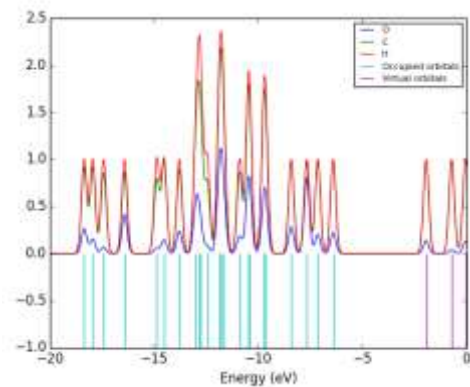


Fig.3 HOMO-LUMO orbitals of UMB molecule





c)

Fig.4a) DOS, **b)** OPDOS and **c)** PDOS of UMB molecule

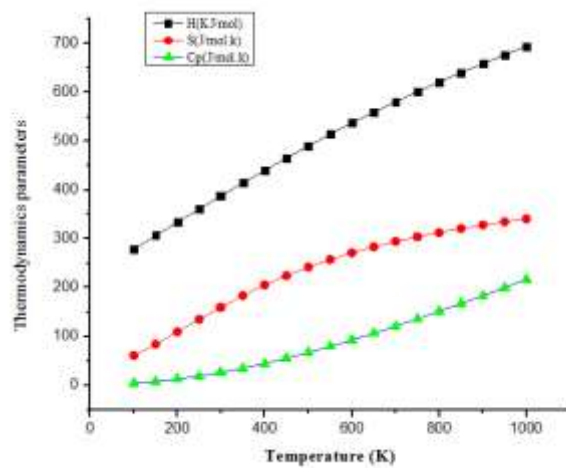


Fig 5. Thermodynamic properties of UMB molecule

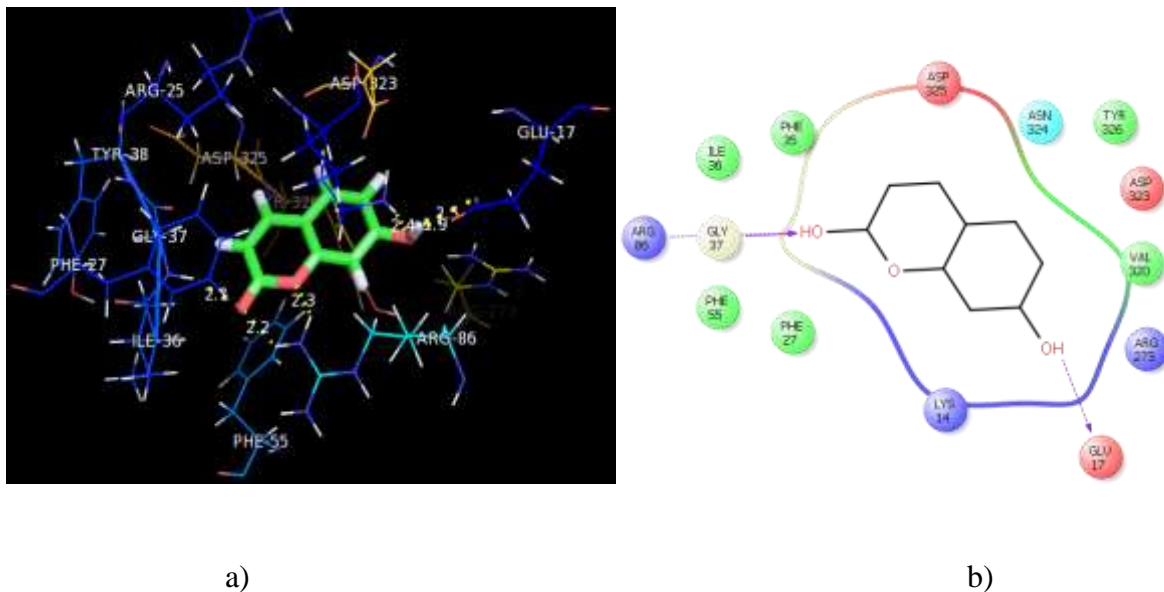


Fig.6 (a,b):The intermolecular interactions formed by umbelliferone molecule in the active Site of PI3K inhibitor

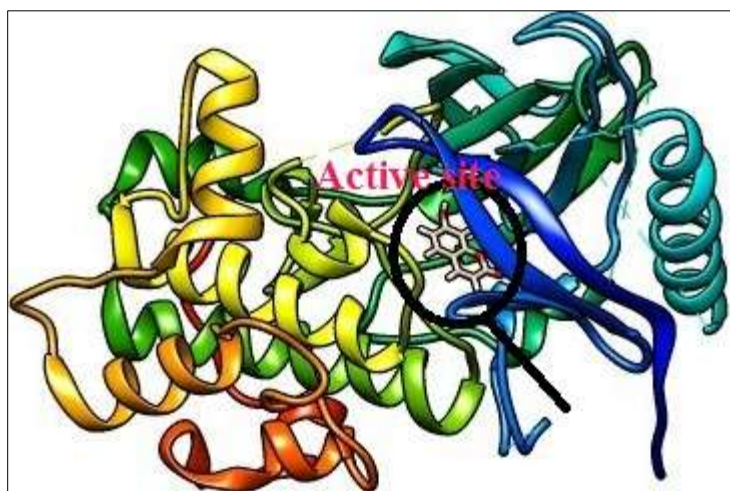


Fig.7 The surface view of umbelliferone molecule binding in the active site of PI3K inhibitor

Table caption

Table 1 Geometrical parameters of UMB

Table 2The molecular descriptors of UMB

Table 3 Fukui values f_k for umbelliferone with Mullikan atomic charges

Table 4 Thermodynamic properties of UMB molecule

Table 5 Lowest binding energy values of UMB molecule in the active site of PI3K

inhibitor in Kcal/mol

Table 6 Nearest neighbor and intermolecular contact distance of UMB molecule in PI3K

inhibitor active site.

Table 1 Geometrical parameters of UMB

Bonds	B3LYP/6-311G(d,p)	HF/6-311G(d,p)
Bond lengths (Å)	DFT	HF
C(1)-C(2)	1.45	1.54
C(1)-O(10)	1.40	1.41
C(1) -O(11)	1.19	1.21
C(2)-C(3)	1.35	1.32
C(2)-H(13)	1.08	1.12
C(3)-C(4)	1.43	1.54
C(3)-H(14)	1.08	1.17
C(4) - C(5)	1.40	1.38
C(4)-C(9)	1.40	1.38
C(5)-C(6)	1.38	1.38
C(5)-H(15)	1.08	1.12
C(6)-C(7)	1.40	1.38
C(6)-H(16)	1.08	1.12
C(7)-C(8)	1.39	1.38
C(7)-O(12)	1.35	1.41
C(8)-C(9)	1.30	1.38
C(8)-H(17)	1.08	1.12
C(9)-O(10)	1.36	1.45
O(12)-H(18)	0.96	0.99
Bond angles (°)		
C(2)-C(1)-O(10)	115.72	120.87
C(2)-C(1)-O(11)	126.76	110.59
O(10)-C(1)-O(11)	117.50	110.59
C(1)-C(2)-C(3)	121.70	111.40
C(1)-C(2)-H(13)	115.54	124.29
C(3)-C(2)-H(13)	122.765	124.29
C(2)-C(3)-C(4)	120.952	120.11
C(2)-C(3)-H(14)	120.34	119.99
C(4)-C(3)-H(14)	118.70	119.99
C(3)-C(4)-C(5)	124.45	119.99
C(3)-C(4)-C(9)	117.50	120.10
C(5)-C(4)-C(9)	118.04	119.99
C(4)-C(5)-C(6)	121.10	120.10
C(4)-C(5)-H(15)	119.03	119.99
C(6)-C(5)-H(15)	119.86	119.99
C(5)-C(6)-C(7)	119.62	120.01
C(5)-C(6)-H(16)	120.42	119.98
C(7)-C(6)-H(16)	119.95	119.98
C(6)-C(7)-C(8)	114 120.62	120.12
C(6)-C(7)-O(12)	122.26	119.98
C(8)-C(7)-O(12)	117.11	119.98
C(7)-C(8)-C(9)	118.98	120.13

C(7)-C(8)-H(17)	120.65	119.98
C(9)-C(8)-H(17)	120.35	119.99
C(4)-C(9)-C(8)	121.61	120.12
C(4)-C(9)-O(10)	121.13	119.68
C(8)-C(9)-O(10)	117.29	119.56
C(1)-O(10)-C(9)	122.98	109.58
C(7)-O(12)-H(18)	109.60	109.50
Torsion angles (°)		
O(10)-C(1)-C(2)-C(3)	0.04	-37.27
O(10)-C(1)-C(2)-H(13)	179.91	143.38
O(11)-C(1)-C(2)-C(3)	-179.95	-168.72
C(2) – C(1)-O(10)-C(9)	-0.10	51.40
O(11)-C(1)-O(10)-C(9)	179.97	-177.03
C(1)-C(2)-C(3)-C(4)	0.01	2.01
C(1)-C(2)-C(3)-H(14)	179.87	-177.46
H(13)-C(2)-C(3)-C(4)	-179.82	-178.66
H(13)-C(2)-C(3)-H(14)	-0.17	1.92
C(2)-C(3)-C(4)-C(5)	179.93	-165.07
C(2)-C(3)-C(4)-C(9)	-0.03	15.42
H(14)-C(3)-C(4)-C(5)	0.14	14.34
H(14)-C(3)-C(4)-C(9)	-179.72	-165.07
C(3)-C(4)-C(5)-C(6)	179.99	-179.47
C(3)-C(4)-C(5)-H(15)	-0.008	1.14
C(9)-C(4)-C(5)-C(15)	179.71	-179.48
C(3)-C(4)-C(9)-C(8)	-179.51	179.42
C(5)-C(4)-C(9)-O(10)	179.99	-179.43
C(4)-C(5)-C(6)-C(7)	-0.01	0
C(4)-C(5)-C(6)-H(16)	179.93	-179.42
H(15)-C(5)-C(6)-C(7)	179.93	179.47
H(15)-C(5) - C(6)-H(16)	-0.04	0
C(5)-C(6)-C(7)-C(8)	0.27	0
C(5)-C(6)-C(7)-O(12)	-179.98	-179.47

H(16)-C(6)-C(7)-C(8)	-179.92	179.71
H(16)-C(6)-C(7)-O(12)	0.04	0
C(6)-C(7)-C(8)-C(9)	-0.23	0
C(6)-C(7)-C(8)-H(17)	-178.949	-179.72
O(12) - C(7)-C(8)-C(9)	-178.76	179.47
O(12)-C(7)-C(8)-H(17)	0.08	0
C(6)-C(7)-O(12)-H(18)	0.12	0
C(8)-C(7)-O(12)-H(18)	-178.93	-179.57
C(7)-C(8)-C(9)-C(4)	-0.034	0
C(7)-C(8)-C(9)-O(10)	-179.94	178.47
H(17)-C(8)-C(9)-C(4)	179.95	178.46

Table 2 The molecular descriptors of UMB

Parameters	B3LYP/6-311G(d,p) Energy (eV)
E_{HOMO}	-9.06649
E_{LUMO}	-5.83779
Band gab $\Delta E = E_{\text{H}} - E_{\text{L}}$	3.2287
Ionization potential(I) $I = [-E_{\text{HOMO}}]$	9.06649
Electron affinity(A) $A = [-E_{\text{LUMO}}]$	5.837790
Electrophilicity $\omega = \mu^2 / 2 \eta$	17.2002
Electro negativity $\chi = (IE + EA) / 2$	7.452142
Global hardness $\eta = (I - A) / 2$	1.61435
Softness $S = 1 / 2 \eta$	0.309721

Table 3 Fukui values f_k for umbelliferone with Mullikan atomic charges

Atoms	Mullikan Atomic Charges			Fukui Function		
	N (0,1)	N+1 (1,2)	N-1 (-1,2)	f+	f-	f0
C1	0.3275	0.4173	0.3203	0.0828	-0.0184	-0.0913
C2	-0.1649	-0.1654	-0.3363	-0.0155	-0.1764	-0.1770
C3	0.2869	0.1967	-0.0197	0.1198	-0.0184	0.1309
C4	-0.1313	-0.1373	-0.14363	-0.0161	-0.0251	-0.0099
C5	-0.0484	-0.0144	-0.1131	0.0394	-0.0647	-0.0966
C6	-0.1254	-0.0471	-0.14876	0.0738	-0.0242	0.1015
C7	0.1818	0.1972	0.1172	0.0254	-0.0675	-0.0739
C8	-0.0618	-0.0161	-0.1242	0.0467	-0.0934	-0.1064
C9	0.1783	0.2331	0.1942	0.0648	0.0437	0.0431
O10	-0.2949	-0.2895	-0.3514	0.0239	-0.0691	-0.0645
O11	-0.2876	-0.1897	-0.4081	0.1242	-0.1214	-0.2254
O12	-0.3893	-0.2547	-0.3817	0.1238	-0.0487	-0.1401
H13	0.13294	0.1919	0.0312	0.0556	-0.0962	0.1548
H14	0.10279	0.1635	0.0162	0.0276	-0.0853	-0.1437
H15	0.0966	0.1541	0.0357	0.0511	-0.0647	0.1291
H16	0.0916	0.1681	0.0332	0.0812	-0.0684	-0.1365
H17	0.1278	0.18182	0.0631	0.0404	-0.0585	0.1615
H18	0.2506	0.2913	0.2295	0.0353	-0.0387	-0.0922

Table 4. Thermodynamic properties of UMB molecule

T(K)	S(J/mol.k)	Cp(J/mol.k)	H(KJ/mol)
100	278	60.458	4.327
150	306.807	83.731	7.918
200	334.335	109.043	12.733
250	361.438	134.799	18.83
298.15	387.262	158.965	25.907
300	388.248	159.87	26.201
350	414.686	183.457	34.792
400	440.619	205.095	44.514
450	465.923	224.609	55.266
500	490.508	242.028	66.94
550	514.316	257.506	79.436
600	537.323	271.28	92.662
650	559.527	283.478	106.536
700	580.942	294.397	120.988
750	601.593	304.188	135.957
800	621.511	313.006	151.391
850	640.73	320.981	167.244
900	659.285	328.222	183.477
950	677.211	334.82	200.055
1000	694.54	340.851	216.949

Table 5 Lowest binding energy values of UMB molecule in the active site of PI3K

inhibitor in Kcal/mol

Ranking	Binding energy
1	-5.98
2	-5.87
3	-5.86

4	-5.68
5	-5.56
6	-5.41
7	-5.40
8	-5.37
9	-5.23
10	-5.13

Table 6 Nearest neighbor and intermolecular contact distance of UMB molecule in PI3K inhibitor active site.

Umbelliferone with PI3K inhibitor amino acid residues	Distance (Å)
O(11)...Gly37/H	2.1
O(11)...Arg86/HH12	2.2
O(10)...Arg86/HH11	2.3
O(12)...Lys14/HZ1	2.4
H(18)...Glu17/OE1	1.9
H(25)...Glu17/OE2	2.5

REFERENCES:

1. H. Surburg, J. Panten, Individual Fragrance and Flavor Materials, in: Common Fragrance and Flavor Materials, Wiley-VCH Verlag GmbH & Co. KGaA, pp. 7-175. (2006)
2. Y. Nakamura, M. Miyamoto, A. Murakami, H. Ohigashi, T. Osawa, K. Uchida, A phase II detoxification enzyme inducer from lemongrass: identification of citral and involvement of electrophilic reaction in the enzyme induction, Biochem. Biophys. Res. Commun. 302 593-600(2003)
3. Haitham AlRabiah, S.Muthu, et.al molecular structure, Macedonian Journal of chemistry and chemical Engineering, Vol 36(2017).

4. KesavanMuthu, K. Gunasekaran, A. Kala, et al. *Int.curr.Microbiol.app.sci* (2015)
5. M. Prasath, M. Govindammal, B. Sathya, *Journal of Molecular Structure*, 1146,292 (2017).
6. M. Ibrahim, A. Aziz Muhmouda, O. Osmana, A. Refaata, M. El-Sayed, *Spectrochim.Acta A* 77 (2010) 802–806
7. M.J. Frisch, G.W. Trucks et al., *Gaussian 09, Revision B.01* (Gaussian Inc., Wallingford, CT, 2010)
8. E. Frisch, H.P. Hratchian, R.D. Dennington II et al., *Gaussview, Version 5.0.8*, 235 (Gaussian Inc., Wallingford, CT,2009)
9. S. Muthu , M. Prasath , R. ArunBalaji ,*SpectrochimicaActa Part A: Molecular and Biomolecular Spectroscopy* 106 (2013) 129–145
10. N.M. O’Boyle, A.L. Tenderholt, K.M. Langner, *J. Comput. Chem.* 29, 839(2008)
11. J.K. Labanowski, J.W. Andzelm, *Density Functional Methods in Chemistry* (Springer, New York,1991)
12. R.G. Parr, W. Yang, *Density Functional Theory of Atoms and Molecules* (Oxford University Press,NewYork,1989)
13. M. Prasath, et al.,*Journal of Cluster Science*,30(4),1025 - 1035(2019).
14. D.F.V. Lewis, C. Ionnadis, D.V. Parke 401(1994).
15. M.Prasath, S Muthu, *Asian Journal of Chemistry.* 25, 6771 (2013)
16. Haitham AlRabiah, S.Muthu, et.al molecular structure, *Macedonian Journal of chemistry and chemical Engineering*, Vol 36(2017)
17. M. Govindammal, M. Prasath, *Heliyon.* 6, e04641 (2020).
18. S. Muthu , M. Prasath , R. ArunBalaji ,*SpectrochimicaActa Part A: Molecular and Biomolecular Spectroscopy* 106 (2013) 129–145
19. SathyaBangaru ,PrasathManivannan , S. Muthu , *Spectroscopicinvestigations, quantum chemical calculations and molecular docking studies of Mangiferin- an anti- viral agent of H1N1 Influenza virus, Chemical Data Collections* (2020)
20. S. Xavier, S. Periandy, K. Carthigayan, S. Sebastian, *J. Mol. Struct.* 1125, 204(2016)
21. P. Kolandaivel, G. Praveen, P. Selvarangan, *Study of atomic and condensed atomic indices for reactive sites of molecules, J. Chem. Sci.* 117, 591–598 (2005).
22. S. Gunasekaran, K. Rajalakshmi, S. Kumaresan, *Spectra chim.Acta Part A* 112,351-353(2013).
23. S. Muthu, E. Isaac Paul raj, *Spectroscopic and molecular structure J. Mol. Struct.* 1038, 145–162 (2013).
24. R.Shahidha, S.Muthu, M. Raja, B. Narayana et.al, *journal of molecular spectroscopy and optic* 140 1127- 1142. (2017)
25. R. Huey, G. M. Morris, A. J. Olson, D. S. Goodsell, *A semiempirical free energy force field with charge-based desolvation, J. Comput. Chem.* 28, 1145–1152 (2007).
26. S. Sevvanthi, S. Muthu, M. Raja, *J. Mol. Str.* 1173, 251(2018)
27. S. Xavier, S. Periandy, K. Carthigayan, S. Sebastian, *J. Mol. Struct.* 1125, 204(2016)

28. V. Arjunan, P.S. Balamourougane, C.V. Mythili, S. Mohan, Journal of Molecular Structure 1003 (2011) 92–102
29. V. Sangeetha , M. Govindarajan , N. Kanagathara , M.K. Marchewka , S. Gunasekaran,G. Anbalagan,SpectrochimicaActa Part A: Molecular and Biomolecular Spectroscopy 118 (2014) 1025–1037
30. S. Dheivamalar, V. Silambarasan,SpectrochimicaActa Part A: Molecular and Biomolecular Spectroscopy 96 (2012) 480–484
31. V. Arjunan, P.S. Balamourougane, C.V. Mythili, S. Mohan, Journal of Molecular Structure 1003 (2011) 92–102
32. S. Prasath, R. ArunBalaji and R. Revathy ,Journal of Chemical and Pharmaceutical Research, 2015, 7(2):213-230